

On the theory of plasma–sheath resonance in a non-uniform plasma

NOBORU TANIZUKA¹ and JOHN E. ALLEN²

¹College of Integrated Arts and Sciences, Osaka Prefecture University,
1-1 Gakuen-cho, Sakai, 599-8531 Japan

²Department of Engineering Science, University of Oxford,
Parks Road, Oxford OX1 3PJ, UK

(Received 24 July 1998 and in revised form 18 January 1999)

Calculations are presented on the phenomenon of plasma–sheath resonance in an inhomogeneous plasma. In certain cases, this resonance coincides with a local resonance occurring in the plasma, the local plasma frequency being equal to the resonant frequency of the entire system. The theory does not describe the mechanism of absorption, but does predict the magnitude of the power involved. Some limitations of the theory are discussed.

1. Introduction

During a programme of research on capacitively coupled radiofrequency (RF) discharges carried out at Oxford, it was found that measurements of the current waveform were not in agreement with the associated theory. It was realized that plasma–sheath resonance was taking place, the resonance being associated with harmonics of the driving frequency of 13.56 MHz (Annaratone et al. 1993). The theory was invalid for the frequencies in question because the electrons were assumed to follow variations in potential without delay (Skorik and Allen 1993; Skorik 1993 personal communication), i.e. the electron inertia was not taken into account. The phenomena of plasma–sheath resonance had been studied in the 1960s with reference to probe measurements (Swift and Schwar 1970), but, as far as we have been able to ascertain, had never been reported in capacitively coupled plasma reactors. Internal probe measurements then revealed the potential distribution due to the plasma–sheath resonance (Ku et al. 1994; Annaratone et al. 1995; Ku 1996). These were made on harmonics of the driving frequency (13.45 MHz), which were generated by the nonlinear response of the space-charge sheaths.

Other recent work on plasma–sheath resonance has been carried out by Matsui et al. (1996, 1997 a–c). The aim of most of this work was to increase the ion extraction from a plasma, the applications being to laser isotope separation and to plasma processing. In the absence of the resonance, the RF electric field is largely screened out of the plasma (Allen and Skorik 1993), but electron inertia effects appear at plasma–sheath resonance when the frequency is comparable to, but less than, the electron plasma frequency. Matsui et al. (1997d) also studied the RF heating of plasmas by means of this resonance, but the actual mechanism was not elucidated.

Returning to the Oxford work, a simple model was at first assumed in which

a uniform plasma existed with boundary sheaths adjacent to the electrodes. To investigate a more realistic situation, a density profile was then assumed to see what effects such a profile would have (Ku et al. 1995, 1998a,b; Allen 1995; Ku 1996). One interesting result was that the plasma–sheath resonance could then coincide with a local plasma resonance. During this work it was found that some relevant theory on non-uniform plasmas had been developed some time ago by Crawford and Harker (1972). A principal result of this theory, which was for cold electrons and no collisions, was that the plasma had a resistive component given by

$$R = \frac{\pi}{\epsilon_0 A \left| \frac{d\omega_{pe}}{dx} \right|},$$

where the derivative is evaluated at the planes where the local resonance takes place. The aim of the present paper is to study this theory in some detail. It is recognized that nonlinear effects may well become important in practice. Other limitations of the theory will be briefly discussed.

2. A model of the plasma–sheath system

The RF-driven plasma reactor is assumed to be simply constituted of two parallel electrodes, the blocking capacitor and the RF power source. The electrodes are circular plates of the same diameter: one is earthed and the other is driven by the power source through the blocking capacitor, which prevents the direct current from flowing through the plasma–sheath system.

The plasma is accompanied by sheaths between the electrode plates and the plasma boundaries. The plasma or the electron density extension along the longitudinal direction is supposed to be confined within a length of $2a$; then the electron density distribution is taken to be one-dimensional and

$$n = \frac{n_0}{1 + (x/a)^2} \quad (-a < x < +a), \quad (1)$$

where n_0 is the maximum plasma electron density at the plasma centre. This form has been assumed by other workers (Bers and Schneider 1968; Crawford and Harker 1972). In this model, the electrons are cold and the ions are insensitive to any electric field of the driving frequency and its higher harmonics.

2.1. Local LC circuit

Consider a thin sheet of thickness δ and area A , and the equivalent parallel connection of a capacitance C and an inductance L . The alternating electric field E , at position x in the x direction, is associated with an alternating voltage of magnitude

$$V = E\delta$$

across the sheet. Let m and e be the mass and charge of an electron and let n be the electron density. The equation of motion $m\dot{v} = -eE$ holds for an electron.

The current carried by electrons through the sheet is given by $I_L = -envA$, and the following equation holds:

$$\begin{aligned} \frac{dI_L}{dt} &= -env\dot{A} \\ &= \frac{e^2 n A E}{m} \\ &= \frac{e^2 n A}{m \delta} V. \end{aligned}$$

Since

$$L \frac{dI_L}{dt} = V$$

holds for the sheet, the equivalent inductance L can be written as

$$L = \frac{m \delta}{n e^2 A}. \tag{2}$$

Introducing the permittivity of free space, ϵ_0 , it is seen that the displacement current flowing through the sheet is given by

$$I_C = A \epsilon_0 \frac{dE}{dt} = \frac{A \epsilon_0}{\delta} \frac{dV}{dt}.$$

The integral of the above equation,

$$\int_0^t I_C dt = \frac{A \epsilon_0}{\delta} V,$$

gives the equivalent capacitance C for the sheet:

$$C = \frac{\delta_0 A}{\delta}. \tag{3}$$

In the particular case of sinusoidal quantities, we can write

$$I = I_L + I_C = \left(\frac{1}{i\omega L} + i\omega C \right) V. \tag{4}$$

2.2. Local impedance

From (4), the local impedance for the sheet is

$$\frac{V}{I} = \frac{i\omega L}{1 - \omega^2 LC}. \tag{5}$$

The resonance of the LC circuit occurs at $\omega = (LC)^{-1/2}$. We call this the *local resonance*. Equations (2) and (3) give

$$\frac{1}{(LC)^{1/2}} = \left(\frac{ne^2}{\epsilon_0 m} \right)^{1/2}, \tag{6}$$

which means that the local resonant frequency is equal to the electron plasma

frequency, i.e. $\omega_{pe}(x)$. Substitution of (1), (2) and (6) into (5) gives the impedance dZ_p of the thin sheath δ :

$$\begin{aligned} dZ_p &= \frac{i\omega}{\epsilon_0 A} \frac{dx}{\omega_{pe}(x)^2 - \omega^2} \\ &= \frac{1}{2i\epsilon_0 A} \left(\frac{1}{\omega - \omega_{pe}(x)} + \frac{1}{\omega + \omega_{pe}(x)} \right) dx, \end{aligned} \quad (7)$$

where δ has been replaced by dx .

Let Ω and γ be respectively the maximum electron plasma frequency, $\omega_{pe}(0)$, and the driving parameter fixing a working condition:

$$\Omega = \left(\frac{n_0 e^2}{\epsilon_0 m} \right)^{1/2}, \quad \gamma = \frac{\Omega}{\omega}.$$

Then we have the following expression for the right-hand side of (7):

$$\begin{aligned} \frac{1}{\omega - \omega_{pe}(x)} + \frac{1}{\omega + \omega_{pe}(x)} &= \frac{1}{\omega} \left(2 + \frac{a\Omega}{\omega(a^2 + x^2)^{1/2} - a\Omega} - \frac{a\Omega}{\omega(a^2 + x^2)^{1/2} + a\Omega} \right) \\ &= \frac{1}{\omega} \left(2 + \frac{2a^2\gamma^2}{x^2 + a^2(1 - \gamma^2)} \right). \end{aligned} \quad (8)$$

2.3. Plasma–sheath system

Substituting from (8) into (7) and integrating dZ_p in the domain $-a < x < a$, the plasma impedance becomes

$$\begin{aligned} Z_p(\gamma) &= \int_{-a}^a dZ_p \\ &= \frac{1}{i\epsilon_0 A \omega} \int_0^a 2 dx + \frac{1}{i\epsilon_0 A \omega} \int_0^a g(x, \gamma) dx, \end{aligned} \quad (9)$$

where we put

$$g(x, \gamma) = \frac{2a^2\gamma^2}{x^2 + a^2(1 - \gamma^2)}. \quad (10)$$

Equation (9) shows that the constant term, 2, represents a capacitive reactance and the variable term, $g(x, \gamma)$, leads to either a capacitive or inductive reactance, depending on the value of γ .

Let s_1 (s_2) be the distance between the plasma boundary $x = a$ ($-a$) and the driven electrode (the earthed electrode). The space of s_1 (s_2) is assumed to be a vacuum; then the plasma and the electrode form the capacitance C_{s_1} (C_{s_2}):

$$C_{s_1} = \frac{\epsilon_0 A}{s_1}, \quad C_{s_2} = \frac{\epsilon_0 A}{s_2}. \quad (11)$$

The total impedance of the plasma–sheath system is then given by

$$\begin{aligned} Z_T(\gamma) &= Z_p(\gamma) + \frac{1}{i\omega} \left(\frac{1}{C_{s_1}} + \frac{1}{C_{s_2}} + \frac{1}{C_{BL}} \right) \\ &= Z_p(\gamma) + \frac{1}{i\omega} \left(\frac{s_1 + s_2}{\epsilon_0 A} + \frac{1}{C_{BL}} \right), \end{aligned} \quad (12)$$

where C_{BL} is the blocking capacitance inserted between the driven electrode

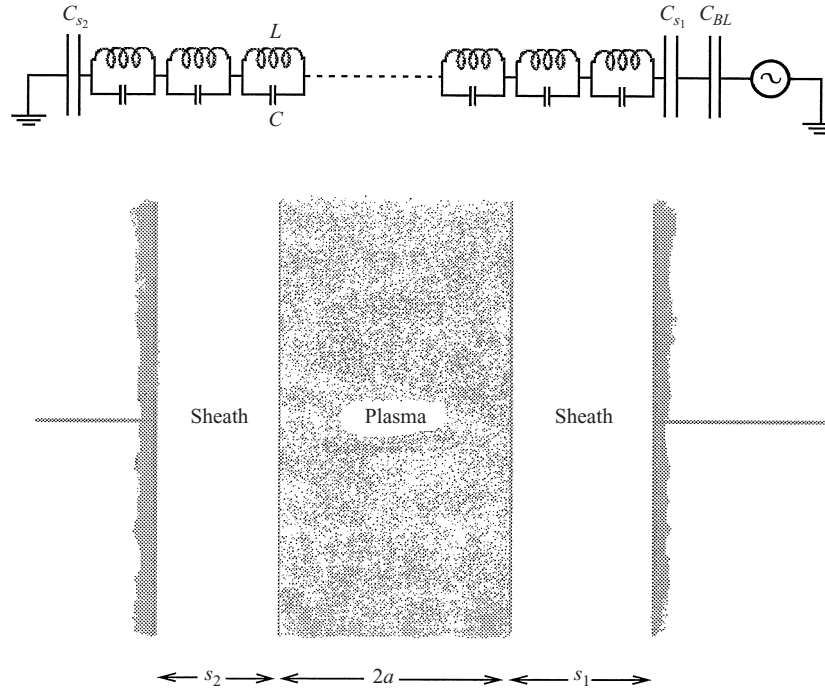


Figure 1. Model of the infinite series of connections of parallel LC circuits for the plasma, together with the circuit model of the total plasma–sheath system.

and the RF power source. The plasma circuit model and the total plasma–sheath system are shown in Fig. 1.

3. Plasma impedance

We put C'_p as

$$C'_p = \frac{\epsilon_0 A}{2a}. \tag{13}$$

By considering the function $g(x, \gamma)$ of (10), the plasma impedance is calculated for the following domains of the parameter γ :

- (i) for $\gamma < 1$: $g(x, \gamma) > 0$, and the reactance is capacitive;
- (ii) for $1 < \gamma < \sqrt{2}$: $g(x, \gamma) < 0$ for $|x| < a(\gamma^2 - 1)^{1/2}$, and the resulting reactance is inductive; $g(x, \gamma) > 0$ for $a(\gamma^2 - 1)^{1/2} < |x| < a$, the reactance is capacitive and we have a pole at $|x| = a(\gamma^2 - 1)^{1/2}$;
- (iii) for $\sqrt{2} < \gamma$: $g(x, \gamma) < 0$, and the reactance is inductive.

The domains are shown in Fig. 2. The maximum and the minimum of the electron plasma frequency are the boundaries for the domains (Fig. 2).

3.1. The domain $\gamma < 1$

The domain $\gamma < 1$ means that the working frequency ω is higher than the maximum plasma frequency Ω . The integral of (10) is given by

$$\int_0^a g(x, \gamma) dx = \frac{2a\gamma^2}{(1 - \gamma^2)^{1/2}} \arctan \frac{1}{(1 - \gamma^2)^{1/2}}.$$

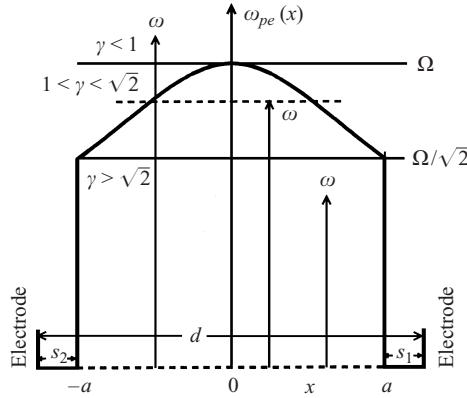


Figure 2. Diagram of the electron plasma frequency and the domains of the parameter γ .

Therefore, from (9), the plasma impedance can be written as

$$Z_p(\gamma) = \frac{1}{i\omega C'_p} \left(1 + \frac{\gamma^2}{(1-\gamma^2)^{1/2}} \arctan \frac{1}{(1-\gamma^2)^{1/2}} \right), \tag{14}$$

where C'_p is given in (13).

From (13) and (14), the effective permittivity of the plasma is given by

$$\epsilon = \frac{\epsilon_0}{1 + \frac{\gamma^2}{(1-\gamma^2)^{1/2}} \arctan \frac{1}{(1-\gamma^2)^{1/2}}}.$$

The permittivity changes as γ , i.e. ω , changes. The plasma impedance for this domain is given by

$$Z_p = \frac{1}{i\omega C'_p}, \tag{15}$$

where

$$C'_p = \frac{\epsilon A}{2a}.$$

The plasma impedance Z_p and the capacitance C'_p are shown in Fig. 3 versus the driving parameter γ .

3.2. The domain $1 < \gamma < \sqrt{2}$

When the working frequency ω enters the domain $1 < \gamma < \sqrt{2}$, the frequency ω is equal to the local plasma frequency at the points $x = \pm a(\gamma^2 - 1)^{1/2}$ (Fig. 2).

Equation (10) can be written as

$$g(x, \gamma) = \frac{a\gamma^2}{(\gamma^2 - 1)^{1/2}} \left(\frac{1}{x - a(\gamma^2 - 1)^{1/2}} - \frac{1}{x + a(\gamma^2 - 1)^{1/2}} \right). \tag{16}$$

The integral of the second term in (16) is

$$\begin{aligned} \int_0^a g_2(x, \gamma) dx &= -\frac{a\gamma^2}{(\gamma^2 - 1)^{1/2}} \int_0^a \frac{1}{x + a(\gamma^2 - 1)^{1/2}} dx \\ &= \frac{a\gamma^2}{(\gamma^2 - 1)^{1/2}} \log \frac{(\gamma^2 - 1)^{1/2}}{1 + (\gamma^2 - 1)^{1/2}}. \end{aligned} \tag{17}$$

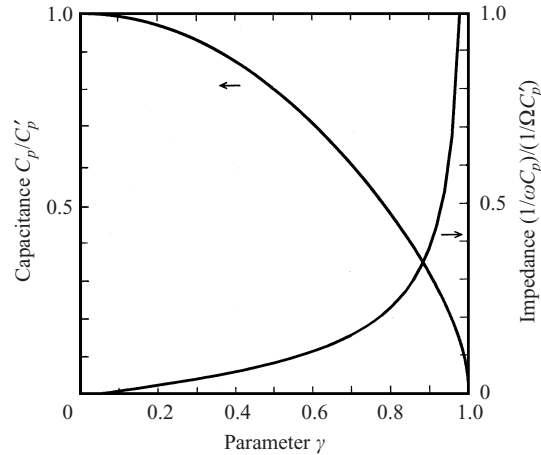


Figure 3. Capacitance C_p and impedance Z_p of the plasma versus the driving parameter γ for the domain $\gamma < 1$.

The integral of the first term in (16) is

$$\int_0^a g_1(x, \gamma) dx = \frac{a\gamma^2}{(\gamma^2 - 1)^{1/2}} \int_0^a \frac{1}{x - a(\gamma^2 - 1)^{1/2}} dx,$$

which has a pole at $x = a(\gamma^2 - 1)^{1/2}$. Then the resulting integral of $g_1(x, \gamma)$ is given by

$$\int_0^a g_1(x, \gamma) dx = \frac{a\gamma^2}{(\gamma^2 - 1)} \left(\log \frac{1 - (\gamma^2 - 1)^{1/2}}{(\gamma^2 - 1)^{1/2}} + \pi i \right). \tag{18}$$

From (9), (10) and (16)–(18), we have the plasma impedance

$$\begin{aligned} Z_p(\gamma) &= \frac{1}{i\omega C'_p} \left[1 + \frac{\gamma^2}{2(\gamma^2 - 1)^{1/2}} \left(\log \frac{1 - (\gamma^2 - 1)^{1/2}}{1 + (\gamma^2 - 1)^{1/2}} + \pi i \right) \right] \\ &= \frac{1}{C'_p} \left[i\omega \frac{\gamma^2}{\Omega^2} \left(\frac{\gamma^2}{2(\gamma^2 - 1)^{1/2}} \log \frac{1 + (\gamma^2 - 1)^{1/2}}{1 - (\gamma^2 - 1)^{1/2}} - 1 \right) + \frac{\pi}{2\Omega} \frac{\gamma^3}{(\gamma^2 - 1)^{1/2}} \right], \end{aligned} \tag{19}$$

where (13) and the equation $\omega = \Omega/\gamma$ have been used.

Let

$$\eta = \frac{\gamma^2}{2(\gamma^2 - 1)^{1/2}} \log \frac{1 + (\gamma^2 - 1)^{1/2}}{1 - (\gamma^2 - 1)^{1/2}}, \tag{20}$$

$$L_p = \frac{1}{C'_p} \frac{\gamma^2}{\Omega^2} (\eta - 1) = \frac{2a\gamma^2}{\epsilon_0 A \Omega^2} (\eta - 1), \tag{21}$$

$$R_p = \frac{1}{C'_p} \frac{\pi}{2\Omega} \frac{\gamma^3}{(\gamma^2 - 1)^{1/2}} = \frac{a\pi}{\epsilon_0 A \Omega} \frac{\gamma^3}{(\gamma^2 - 1)^{1/2}}, \tag{22}$$

where

$$\eta > 1 \quad \text{and} \quad \lim_{\gamma \rightarrow 1} \eta = 1.$$

Then, from (19), the plasma impedance can be written as

$$Z_p = i\omega L_p + R_p. \tag{23}$$

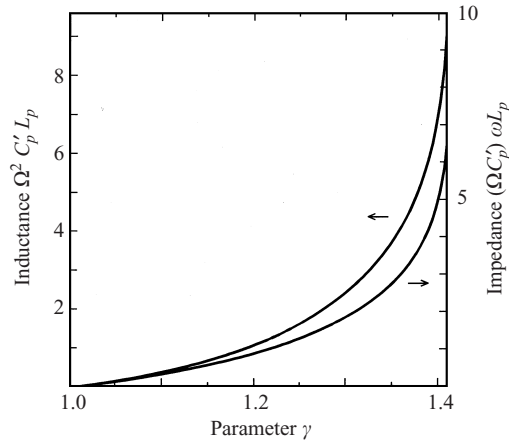


Figure 4. Inductance L_p and reactance ωL_p of the plasma versus the driving parameter γ for the domain $1 < \gamma < \sqrt{2}$.

The plasma inductance L_p and the reactance ωL_p are shown in Fig. 4 versus the driving parameter γ . The resistance R_p is shown in Fig. 8 below.

3.3 The domain $\gamma > \sqrt{2}$

When the working frequency ω is less than the minimum plasma frequency, i.e. $\omega < \Omega/\sqrt{2}$, $g(x, \gamma) < 0$ in every coordinate of the plasma ($|x| < a$). The integral of $g(x, \gamma)$ gives

$$\begin{aligned} \int_0^{a_0} g(x, \gamma) dx &= \int_0^a \frac{a\gamma^2}{(\gamma^2-1)^{1/2}} \left(\frac{1}{x-a(\gamma^2-1)^{1/2}} - \frac{1}{x+a(\gamma^2-1)^{1/2}} \right) dx \\ &= \frac{a\gamma^2}{(\gamma^2-1)^{1/2}} \log \frac{(\gamma^2-1)^{1/2}-1}{(\gamma^2-1)^{1/2}+1}. \end{aligned} \quad (24)$$

Using (9) and (13), the plasma impedance can be written as

$$Z_p(\gamma) = \frac{1}{i\omega C_p'} \left(1 + \frac{\gamma^2}{2(\gamma^2-1)^{1/2}} \log \frac{(\gamma^2-1)^{1/2}-1}{(\gamma^2-1)^{1/2}+1} \right) \quad (25)$$

$$= \frac{1}{C_p'} \left[i\omega \frac{\gamma^2}{\Omega^2} \left(\frac{\gamma^2}{2(\gamma^2-1)^{1/2}} \log \frac{(\gamma^2-1)^{1/2}+1}{(\gamma^2-1)^{1/2}-1} - 1 \right) \right], \quad (26)$$

where $\omega = \Omega/\gamma$ has been used.

Let

$$\xi = \frac{\gamma^2}{2(\gamma^2-1)^{1/2}} \log \frac{(\gamma^2-1)^{1/2}+1}{(\gamma^2-1)^{1/2}-1}, \quad (27)$$

$$L_p = \frac{1}{C_p'} \frac{\gamma^2}{\Omega^2} (\xi - 1) = \frac{2a\gamma^2}{\epsilon_0 A \Omega^2} (\xi - 1). \quad (28)$$

Then the plasma impedance in this domain can be written as

$$Z_p = i\omega L_p \quad (29)$$

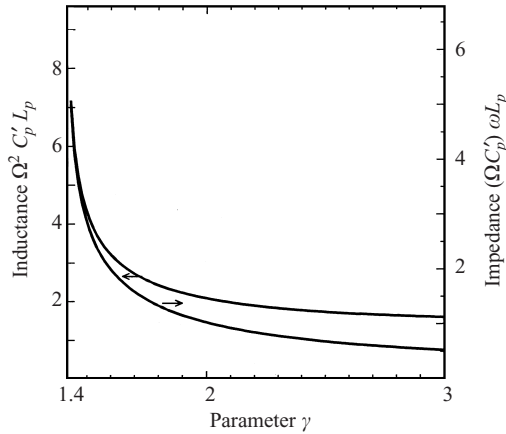


Figure 5. Inductance L_p and impedance Z_p of the plasma versus the driving parameter γ for the domain $\gamma > \sqrt{2}$.

The plasma inductance L_p and impedance Z_p are shown in Fig. 5 versus the driving parameter γ . Because $\xi > 1$ in this domain, the plasma acts as an inductance.

4. Overall impedance

The impedance of the plasma–sheath system is given by replacing $Z_p(\gamma)$ in (12) with the plasma impedance Z_p for each domain of the driving parameter γ . Typical values of s_1 , s_2 , A and C_{BL} in experiments in our laboratory are $s_1 + s_2 \geq 1$ cm, $A \approx 10^{-2}$ m² and $C_{BL} \approx 0.1$ μ F; then the sheath capacitance

$$C_s = \frac{\epsilon_0 A}{s_1 + s_2} \leq 10 \text{ pF} \tag{30}$$

is less than 10^{-4} times the blocking capacitance: $C_s/C_{BL} \leq 10^{-4}$. Then, from (12), the total impedance can be written as

$$\begin{aligned} Z_T(\gamma) &= Z_p(\gamma) + \frac{1}{i\omega} \frac{s_1 + s_2}{\epsilon_0 A} \\ &= Z_p(\gamma) + \frac{1}{i\omega C_s}. \end{aligned} \tag{31}$$

4.1. The domain $\gamma < 1$

Substituting Z_p from (15) for $Z_p(\gamma)$ in (31), we have

$$\begin{aligned} Z_T(\gamma) &= \frac{1}{i\omega} \left(\frac{1}{C_p} + \frac{1}{C_s} \right) \\ &= \frac{1}{i\omega} \left(\frac{1}{C_{ED}} + \frac{1}{C'_p} \frac{\gamma^2}{(1-\gamma^2)^{1/2}} \arctan \frac{1}{(1-\gamma^2)^{1/2}} \right), \end{aligned} \tag{32}$$

where

$$C_{ED} = \frac{\epsilon_0 A}{d},$$

with

$$d = s_1 + s_2 + 2a \quad (\text{distance between the electrodes}), \quad (33)$$

has been used. C_{ED} is equivalent to the capacitance formed by the driven and earthed electrodes with a vacuum space. The total impedance is capacitive in this domain of the parameter γ .

4.2. The domain $1 < \gamma < \sqrt{2}$

Substituting (23) for $Z_p(\gamma)$ in (31), we have

$$Z_T(\gamma) = i\omega L_p + \frac{1}{i\omega C_s} + R_p \quad (34)$$

$$= \frac{1}{\omega C_p'} \left[\left(\eta - 1 - \frac{s_1 + s_2}{2a} \right) i + \frac{\pi\gamma^2}{2(\gamma^2 - 1)^{1/2}} \right], \quad (35)$$

where (13) and (20)–(22) have been used. The expression $\omega(\gamma/\Omega)^2$ can be used in place of $1/\omega$ in (35).

4.3. The domain $\gamma > \sqrt{2}$

Substituting (29) for $Z_p(\gamma)$ in (31), we have

$$Z_T(\gamma) = i\omega L_p + \frac{1}{i\omega C_s} \quad (36)$$

$$= \frac{i}{\omega C_p'} \left(\xi - 1 - \frac{s_1 + s_2}{2a} \right), \quad (37)$$

where (27) and (28) have been used. The total impedance for this domain is given by (37). The expression $1/\omega$ in (37) can be replaced by $\omega(\gamma/\Omega)^2$.

5. Overall resonance

When the plasma–sheath system is driven at the series resonant frequency, the reactance of the system is zero. The overall resonance condition is written as

$$\text{Im } Z_T(\gamma) = 0. \quad (38)$$

5.1. The domain $\gamma < 1$

From Sec. 4.1 and (38), there is no overall resonance in this domain.

5.2. The domain $1 < \gamma < \sqrt{2}$

From Sec. 4.2 and (38), the resonant condition for the plasma–sheath system in this domain is

$$\eta = 1 + \frac{s_1 + s_2}{2a} = \frac{d}{2a}, \quad (39)$$

where η is given by (20), and d is the distance between the electrodes,

$$d = s_1 + s_2 + 2a.$$

The total impedance at overall resonance is the resistance R_p given in (22).†

† The process by which the RF power is absorbed in the plasma through the resistance R_p is an open question (Crawford and Harker 1972).

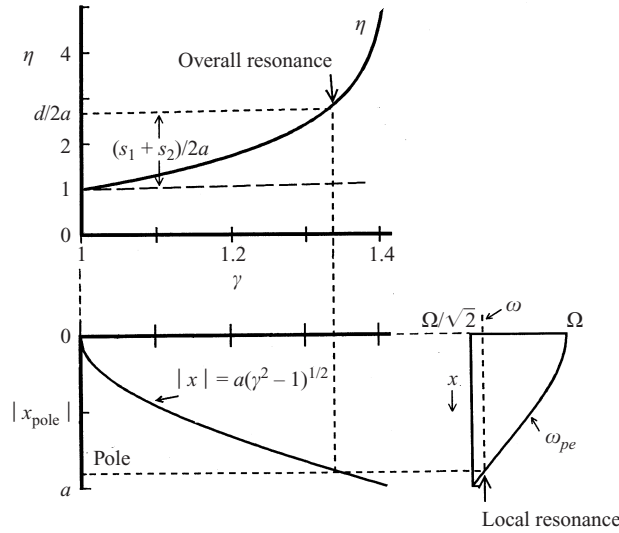


Figure 6. Overall resonance occurs when the ratio of the distance between the two electrodes to the plasma length is equal to η . At the same time, local resonance occurs at the poles.

Equation (39) tells us that an overall resonant condition depends upon the ratio of the distance between the electrodes to the plasma length. This means that the driving parameter $\gamma = \Omega/\omega$ on which η depends, (20), fixes the ratio $d/2a$ and $(s_1 + s_2)/2a$, when the system is driven at the overall resonant frequency.‡ At the pole positions $x = \pm a(\gamma^2 - 1)^{1/2}$, local resonances occur simultaneously; the poles analytically yielded a value for the resistance in Sec. 3.2. A plot of overall and local resonances is shown schematically in Fig. 6.

5.2.1. *Q of plasma-sheath system.* A voltage amplification factor for the sheaths can be defined as

$$A_s = \frac{\text{RF voltage across the sheaths at resonance}}{\text{total RF voltage across the system}}.$$

Then

$$A_s = \frac{1}{\omega C_s R_p} = \frac{\omega L_p}{R_p};$$

this quantity resembles the Q factor for a simple LCR circuit, but in the present case both L_p and R_p are functions of frequency. For this reason, we define Q using the relation

$$\frac{\text{half-power bandwidth}}{\omega} = \frac{1}{Q}.$$

The voltage amplification factor A_s is shown in Fig. 7 versus the parameter γ . Let F be the normalized driving frequency:

$$F = \frac{\omega}{\Omega} = \frac{1}{\gamma}.$$

‡ The ratio can be chosen so that the system is driven at the overall resonant frequency.

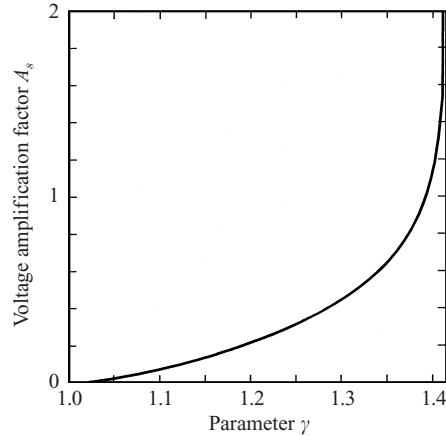


Figure 7. Voltage amplification factor for the sheaths, A_s , versus the parameter γ .

We calculate the current $I(F)$ and the power $P(F)$ absorbed by the plasma corresponding to the change in the driving frequency F :

$$\begin{aligned}
 I(F) &= \frac{V_{RF}}{|Z_T(F)|}, \\
 P(F) &= R_p I^2(F) \\
 &= \frac{2\pi\Omega C_p' V_{RF}^2 F^2 (1-F^2)^{1/2}}{\left(\log \frac{F + (1-F^2)^{1/2}}{F - (1-F^2)^{1/2}} - 2\beta F (1-F^2)^{1/2}\right)^2 + \pi^2}, \quad (40)
 \end{aligned}$$

where (22) and (35), $\gamma = F^{-1}$ and the parameter

$$\beta = d/2a$$

have been used; V_{RF} is the (r.m.s.) RF voltage.

$P(F)$ and R_p are shown in Fig. 8 as functions of the normalized driving frequency F , and $P(F)$ in units of $2\pi\Omega C_p' V_{RF}^2$.

Q of the plasma–sheath system can be calculated in terms of the frequency F_0 at which the power is maximum and the frequencies F_1 and F_2 ($F_1 < F_2$) at which the power is half maximum:

$$Q = \frac{F_0}{F_2 - F_1}. \quad (41)$$

In Table 1, the numerically calculated value of Q is given for each fixed value of β ($\beta = 1.329$ and 1.588 are the values used in Tables 2–4). In Table 1, the errors for F_0 , $F_2 - F_1$ and Q are $\Delta F_0 = \pm 0.012$, $\Delta(F_2 - F_1) = \pm 0.002$ and $\Delta Q = \pm 0.05$ respectively. $\beta - 1$ and γ_0 are given by

$$\beta - 1 = \frac{s_1 + s_2}{2a}, \quad \gamma_0 = F_0^{-1};$$

$\eta_0 \neq \beta$, so that the condition (38) is not satisfied at the frequency F_0 . The maximum power occurs near but not at the plasma–sheath resonant frequency.

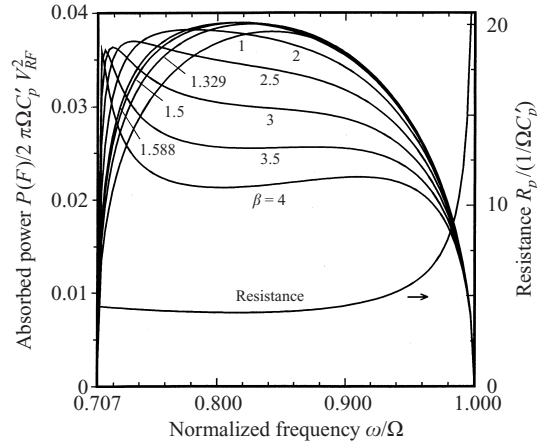


Figure 8. Calculated power absorbed by the plasma, $P(F)$, and the resistance appearing at the poles, R_p , versus the normalized driving frequency $F = \omega/\Omega$. The value of the ratio β of the distance between the driven and earthed electrodes to the plasma length is shown next to each curve.

Table 1. The parameter β used in the simulations, the frequency F_0 at which the power is maximum, the half-power bandwidth $F_2 - F_1$, and the value of Q calculated from (41). η_0 is the value given by (20) for $\gamma = \gamma_0$.

β	1	1.329	1.5	1.588	2	2.5	3	3.5	4
F_0	0.850	0.840	0.833	0.833	0.810	0.782	0.750	0.732	0.721
$F_2 - F_1$	0.262	0.264	0.264	0.265	0.265	0.268	0.270	0.270	—
Q	3.24	3.18	3.16	3.15	3.05	2.91	2.78	2.71	—
$\beta - 1$	0	0.329	0.5	0.588	1	1.5	2	2.5	3
γ_0	1.176	1.190	1.200	1.200	1.235	1.279	1.333	1.366	1.387
η_0	1.616	1.683	1.734	1.734	1.931	2.239	2.786	3.334	3.924

It can be noted that both the plasma resistance and the plasma inductance are frequency-dependent. Thus the usual analysis of a simple LCR circuit, with constant circuit parameters, cannot be expected to apply in the present case.

We note that in the numerical calculation we fixed the value of β , which is the ratio of the gap d to the plasma length, as we changed the driving frequency; however, in reality β cannot be controlled or fixed as the driving frequency is changed. In spite of this, the experimental data on Q for the plasma–sheath system show values of this order (Annaratone et al. 1996).

In Fig. 9, Q is shown as a function of $\beta - 1$, which is equal to $(s_1 + s_2)/2a$, the fixed ratio of the total sheath length to the plasma length. At high values of β , as shown in Fig. 8, the $P(F)$ curve distorts too much to yield a value of Q .

5.2.2. Power absorption in the plasma. At the overall resonance, the total impedance is only the resistance R_p that appears at the poles $x = \pm a(\gamma^2 - 1)^{1/2}$:

$$Z_T(\gamma) = R_p. \tag{42}$$

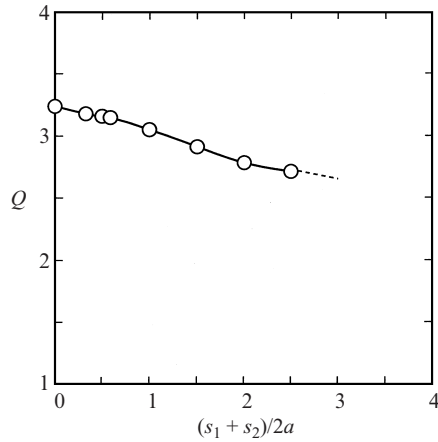


Figure 9. Q of the plasma–sheath system versus the ratio of the total sheath length to the plasma length.

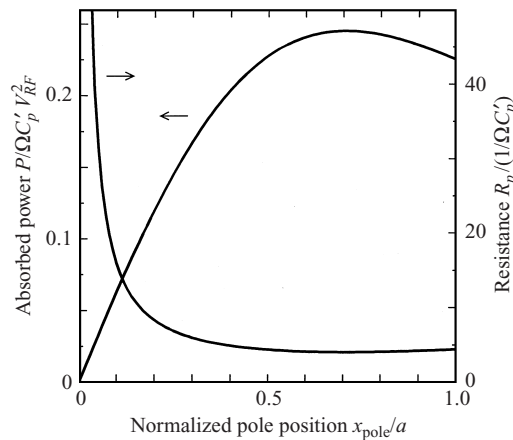


Figure 10. Plasma resistance and the power absorbed by the plasma versus the normalized pole position.

The power absorbed by the plasma can be written as

$$\begin{aligned}
 P &= \frac{V_{RF}^2}{R_p} \\
 &= \frac{\epsilon_0 A \Omega (\gamma^2 - 1)^{1/2}}{a \pi \gamma^3} V_{RF}^2 \\
 &= \frac{\epsilon_0 A \Omega}{a \pi} \frac{|x_{n,pole}|}{(x_{n,pole}^2 + 1)(x_{n,pole} + 1)^{1/2}} V_{RF}^2, \tag{43}
 \end{aligned}$$

where

$$x_{n,pole} = \pm (\gamma^2 - 1)^{1/2}. \tag{44}$$

$x_{n,pole} = x_{pole}/a$ is the normalized pole position.

Figure 10 shows the resistance R_p and the power P absorbed by the plasma versus the normalized pole position $x_{n,pole}$.

5.3. The domain $\gamma > \sqrt{2}$

Because $\xi > 1$ for this domain, the overall resonance can occur under the condition

$$\xi = 1 + \frac{s_1 + s_2}{2a} = \frac{d}{2a} \quad (45)$$

from (37), where ξ is given by (27). However, note that the plasma resistance is theoretically zero for this domain of γ .

When the system is driven at a value of γ such that (45) no longer holds, it operates inductively for higher frequencies, with an impedance

$$Z_T(\omega) = i\omega \frac{\gamma^2}{C_p' \Omega^2} \left(\xi - \frac{d}{2a} \right), \quad (46)$$

and operates capacitively for lower frequencies, with an impedance

$$Z_T(\omega) = \frac{1}{i\omega C_p'} \left(\frac{d}{2a} - \xi \right). \quad (47)$$

6. Discussion and conclusions

We have obtained analytical solutions for the impedance of the plasma for the given electron density distribution. The result is as follows:

- (i) for the domain where the working frequency ω is greater than the maximum electron plasma frequency Ω , $\omega > \Omega$ ($\gamma < 1$), the plasma acts as a capacitance;
- (ii) for the domain where ω is less than Ω but larger than $\Omega/\sqrt{2}$ ($1 < \gamma < \sqrt{2}$), the plasma acts as an inductance and resistance in series;
- (iii) for the domain where ω is less than $\Omega/\sqrt{2}$ ($\gamma > \sqrt{2}$), the plasma behaves as an inductance.

Each impedance for the plasma is an explicit function of γ or ω , which enables us to apply it to a real plasma–sheath system.

In domains (ii) and (iii), the plasma–sheath system can work at overall resonance under suitable conditions, because of the sheaths, which act as capacitances. The difference between the resonances in the domains (ii) and (iii) is that in (ii) there are resistive planes in the plasma at which the power is absorbed, while in (iii) there is no resistive plane. In the case of (iii) an effective large current flow may flow under the resonance condition because of zero theoretical plasma resistance; however, in this case, the mechanism of power absorption must be intrinsically different from that in the case of (ii) and is not covered by the present theory.

6.1. Application to a real system

In this subsection, the analytical solutions will be applied to a real system. Typical quantities for a real plasma–sheath system are as follows:

$$\begin{aligned} \text{RF frequency} \quad f &= 13.56 \text{ MHz}, \\ \text{RF voltage} \quad V_{RF} &= 100 \text{ V (r.m.s.)}, \\ \text{maximum electron density} \quad n_0 &= 5.0 \times 10^{13} \text{ m}^{-3}, \end{aligned}$$

plasma length $2a = 0.10$ m,

plasma diameter $D = 0.10$ m,

area of plasma cross-section $A = \frac{1}{4}\pi D^2 = 2.5\pi \times 10^{-3}$ m²,

maximum plasma frequency $\frac{\Omega}{2\pi} = 63.48$ MHz

capacitance $C'_p = \frac{\epsilon_0 A}{2a} = 0.695$ pF,

inductance $\frac{1}{C'_p \Omega^2} = 9.04$ μ H,

impedance $\frac{1}{C'_p \Omega} = 3.60 \times 10^3$ ohm.

The capacitance, inductance, resistance and impedance of the plasma can be estimated for the typical quantities by using C'_p (0.695 pF), $1/C'_p \Omega^2$ (9.04 μ H) and $1/C'_p \Omega$ (3.60×10^3 ohm) together with Figs 3–5 and 8.

The maximum resistance $R_{p,\min}$ and the maximum power P_{\max} are obtained at $\gamma = \sqrt{\frac{3}{2}}$ and $x_{n,\text{pole}} = \pm \sqrt{\frac{1}{2}}$ from (22) and (43) respectively:

$$R_{p,\min} = \frac{3a\pi}{2eA} \left(\frac{3m}{\epsilon_0 n_0} \right)^{1/2},$$

$$P_{\max} = \frac{2eA}{3a\pi} \left(\frac{\epsilon_0 n_0}{3m} \right)^{1/2} V_{RF}^2.$$

The minimum resistance and the maximum power for the typical quantities given above are

$$R_{p,\min} = 1.47 \times 10^4 \text{ ohm}, \quad P_{\max} = 0.680 \text{ W}.$$

The large minimum resistance and the small maximum power are the theoretical results.

6.2. Predictions of the theory for some experimental parameters

When experiments are carried out with a RF-driven parallel-plate plasma reactor, measurements are made of the sheath thicknesses s_1 and s_2 and the potential distribution along the perpendicular x axis. The potential distribution is expected to go up at the poles.

Empirically, the k th orders of higher harmonics are to be found ($k = 1, 2, 3, \dots$). When the system is operating at the k th order, the working frequency ω and the driving parameter γ are given by

$$\omega = 2\pi f k,$$

$$\gamma = \frac{\Omega}{2\pi f k}$$

$$= \frac{4.68}{k} \quad \text{for the set of figures given above.} \quad (48)$$

Table 2. Typical plasma characteristics for the fundamental frequency and higher (k th) harmonics.

k	1	2	3	4	5	6
γ	4.68	2.34	1.56	1.17	0.936	0.78
Domain		$\gamma > \sqrt{2}$		$\sqrt{2} > \gamma > 1$		$\gamma < 1$
$\omega/2\pi$ (MHz)	13.56	27.12	40.68	54.24	67.80	81.36
Plasma		Inductive		Inductive and resistive		Capacitive
L_p, R_p, C_p	12.9 μ H	16.3 μ H	31.9 μ H	7.28 μ H and 14.9 kohm	0.170 pF	0.350 pF

Table 3. Overall resonance for the fundamental frequency and higher (k th) harmonics.

k	1	2	3	4
γ	4.68	2.34	1.56	1.17
Domain		$\gamma > \sqrt{2}$		$\sqrt{2} > \gamma > 1$
$d/2a$	1.065	1.329	2.449	1.588
A_s		—		0.166
(i) Plasma length $2a = 100$ mm				
d (mm)	107	133	245	159
P (W), x_{pole} (mm)		No pole		0.68, ± 30.4
$s_1 + s_2$ (mm)	6.5	32.9	145	58.8
(ii) Interelectrode length $d = 120$ mm				
$2a$ (mm)	112.6	90.3	49.0	75.6
P (W), x_{pole} (mm)		No pole		0.65, ± 22.9
$s_1 + s_2$ (mm)	7.3	29.7	71.0	44.4

In Table 2, the values of the parameter γ corresponding to each of the higher harmonics are given for the typical quantities of the plasma–sheath system considered here (see Sec. 6.1); the domains of γ and the values of capacitance, resistance and inductance of the plasma are also given.

In Table 3, the ratio $d/2a$ from (39) and (45) is given for each value of γ . A_s , P , x_{pole} and $s_1 + s_2$ are given for each value of γ under the overall resonant operation for the two cases of (i) the plasma length fixed at $2a = 100$ mm and (ii) the interelectrode length fixed at $d = 120$ mm. The total sheath thickness $s_1 + s_2$ is also given. In fact, it is this sum $s_1 + s_2$ that determines the resonant frequency.

The plasma length will be fixed at one of the values such that the plasma–sheath system has an overall resonant frequency satisfying (39) or (45) (different plasma lengths: see Table 3(ii)).

Examples of choosing and setting the plasma length at a fixed value of $d/2a$ are shown in Table 4 for two cases; (i) $d/2a = 1.329$ ($2a = 90.3$ mm), when the overall resonant frequency is 27.12 MHz ($k = 2$), and (ii) $d/2a = 1.588$ ($2a = 75.6$ mm), when the overall resonant frequency is 54.2 MHz ($k = 4$). Overall resonance was not obtained for $k = 1, 3$ and 4 in case (i) or for $k = 1, 2$ and 3 in case (ii); the reactance remains finite at these frequencies in both cases. Table 4 shows that there are coincident local and overall resonances at different harmonics in case (i), and coincident local and overall resonances at the same harmonic in case (ii).

Table 4. Tuning of the k th harmonics for a fixed interelectrode distance, $d = 120$ mm.

k	1	2	3	4
γ	4.68	2.34	1.56	1.17
(i) $d/2a = 1.329$				
$Z_T(\omega)$ (kohm)	$-4.01i$ Capacitive	0	$5.67i$ Inductive	$0.98i + 13.4$ Inductive and resistive
x_{pole} (mm)		—		± 27.4
Resonance	None	Overall	None	Local
(ii) $d/2a = 1.588$				
$Z_T(\omega)$ (kohm)	$-9.09i$ Capacitive	$-2.25i$	$4.99i$ Inductive	14.5 Resistive
x_{pole} (mm)		—		± 22.9
Resonance		None		Local and overall

6.3. Limitations of the theory

The limitations of the theory described in this paper are clear. A one-dimensional plasma has been considered in which the electrons are cold and there are no collisions. The electrons are localized in space, and crossover of trajectories cannot occur; the electron plasma frequency is a function of the space coordinate, and this function is assumed to be time-independent. Furthermore, the theory is a linear one; as it predicts energy absorption in vanishingly small regions of space, one would expect nonlinear phenomena to develop. Although the present theory has its limitations, it does predict energy absorption in the plasma at the planes where the local plasma frequency is equal to the plasma–sheath resonant frequency, i.e. the resonant frequency of the whole system. Possible mechanisms for the absorption of energy in the real case include collisions or the excitation of plasma waves, which can carry energy away from the resonance region.

Recent experiments by Annaratone et al. (1997) and Dyson et al. (1998) have revealed a double layer separating two different regions of the plasma, the inner one being much brighter than the outer. The tentative explanation was to identify this region with the local resonance, suggesting that the strong localized RF electric field produces a localized DC field, somewhat akin to the RF enhanced sheath that develops at the electrodes of any capacitively coupled plasma reactor (Braithwaite et al. 1985). Evidence for a DC potential drop was obtained by measuring the ion energy distribution at the earthed electrode; this was found to show two peaks, one associated with the inner plasma and the other emanating from the outer weaker plasma. Clearly, more experimental work is required to verify these ideas. A new plasma reactor may well result from this work – if not, it will at least provide the basis for a very useful diagnostic that can be widely employed in the laboratory and in the microelectronics industry.

Acknowledgements

The authors wish to thank Dr Beatrice Annaratone and Dr Victor Ku for many detailed discussions concerning the discovery of the plasma–sheath resonance in a plasma reactor and the associated theory for a non-uniform plasma. This

research was carried out while one of the authors (N.T.) worked as a Zaigai Kenkyuin (research worker abroad) supported by a grant from Osaka Prefecture, Japan.

Appendix

The integrals evaluated in this paper involve functions that have poles in the complex plane. There are two ways of determining the correct path of integration: one is to examine the sign of the energy absorbed, since this must be a positive quantity, the other is to consider an initial-value problem and employ the Laplace transform (Crawford and Harker 1972). The second method is to be preferred, since it yields the result for the final steady state as $t \rightarrow \infty$.

References

- Annaratone, B. M., Ku, V. P. T. and Allen, J. E. 1993 In: *Proceedings of International Conference on Phenomena in Ionized Gases* (ed. G. Ecker, U. Arendt and J. Böseler), Vol. I, p. 31. Arbeitsgemeinschaft Plasmaphysik, Bochum.
- Annaratone, B. M., Ku, V. P. T. and Allen, J. E. 1995 *J. Appl. Phys.* **77**, 5455.
- Annaratone, B. M., Allen, J. E., Law, D. A. and Steel, W. H. 1996 In: *Proceedings of XIII ESCAMPIG* (ed. G. Thomas). *Europhys. Conf. Abstr.*, Vol. 20E, p. 173. European Physics Society, Poprad, Slovakia.
- Annaratone, B. M., Allen, J. E. and Dyson, A. E. 1997 *Proceedings of International Conference on Phenomena in Ionized Gases* (ed. M. C. Bordage and A. Gleizes), Vol. I, p. 116. Université Paul Sabatier, Toulouse.
- Allen, J. E. 1995 In: *Phenomena in Ionized Gases* (ed. K. H. Becker, W. E. Carr and E. E. Kunhardt). *AIP Conf. Proc.*, Vol. 363, p. 316. AIP Press, Hoboken, NJ.
- Allen, J. E. and Skorik, M. A. 1993 *J. Plasma Phys.* **50**, part 2, 243.
- Bers, A. and Schneider, H. M. 1968 *MIT Rep.* **89**, 123; **91**, 118.
- Braithwaite, N. St. J., Crosby, A. J. and Allen, J. E. 1985 In: *Proceedings of 8th International Conference on Gas Discharges and their Applications*, p. 482. Leeds University Press.
- Crawford, F. W. and Harker, K. J. 1972 *J. Plasma Phys.* **8**, 261.
- Dyson, A. E., Annaratone, B. M. and Allen, J. E. 1998 In: *Proceedings of XIV ESCAMPIG. Europhys. Conf. Abstr.* Vol. 22H, p. 204.
- Ku, V. P. T. 1996 Experimental studies of capacitively coupled RF discharges. DPhil thesis, University of Oxford.
- Ku, V. P. T., Annaratone, B. M. and Allen, J. E. 1994 In: *Proceedings of XII ESCAMPIG*, Vol. 18E, p. 167. Leeuwenhorst, Noordwijkerhout, The Netherlands.
- Ku, V. P. T., Annaratone, B. M. and Allen, J. E. 1995 In: *Proceedings of International Conference on Phenomena in Ionized Gases* (ed. K. H. Becker, W. E. Carr and E. E. Kunhardt), Vol. IV, p. 157. Stevens Institute of Technology, Hoboken, NJ.
- Ku, V. P. T., Annaratone, B. M. and Allen, J. E. 1998a *J. Appl. Phys.* **84**, 6536.
- Ku, V. P. T., Annaratone, B. M. and Allen, J. E. 1998b *J. Appl. Phys.* **84**, 6546.
- Matsui, T., Tsuchida, K. and Tsuda, S. 1996 *Phys. Plasmas* **3**, 4367.
- Matsui, T., Tsuchida, K., Tsuda, S., Suzuki K. and Shoji, T. 1997a *J. Nucl. Sci. Technol.* **34**, 923.
- Matsui, T., Tsuchida, K., Tsuda, S., Suzuki, K. and Shoji, T. 1997b *Phys. Plasmas* **4**, 3518.
- Matsui, T., Tsuda, S., Tsuchida, K., Suzuki, K. and Shoji, T. 1997c *Phys. Plasmas* **4**, 3527.
- Matsui, T., Tsuda, S. and Yamada, K. 1997d In: *Proceedings of International Conference on Phenomena in Ionized Gases* (ed. M. C. Bordage and A. Gleizes), Vol. I, p. 142. Université Paul Sabatier, Toulouse.

Skorik, M. A. and Allen, J. E. 1993 In: *Proceedings of International Conference on Phenomena in Ionized Gases* (ed. G. Becker, U. Arendt and J. Bösel), p. 113. Arbeitsgemeinschaft Plasmaphysik, Bochum.

Swift, J. D. and Schwar, M. J. R. 1970 *Electrical Probes for Plasma Diagnostics*, p. 156. Iliffe Books, London.